Cell

Transgenerational Stability of the *Arabidopsis* Epigenome Is Coordinated by CG Methylation

Olivier Mathieu,[1,2,*] Jon Reinders,[1] Marian Čaikovski,[1] Chotika Smathajitt,[1] and Jerzy Paszkowski[1,*]
[1]Laboratory of Plant Genetics, University of Geneva, Sciences III, 30 Quai Ernest-Ansermet, CH-1211 Geneva 4, Switzerland
[2]Centre National de la Recherche Scientifique, UMR 6547, Université Blaise Pascal, 24 Avenue des Landais, 63177 Aubière Cedex, France
*Correspondence: olivier.mathieu@univ-bpclermont.fr (O.M.), jerzy.paszkowski@bioveg.unige.ch (J.P.)
DOI 10.1016/j.cell.2007.07.007

SUMMARY

Maintenance of CG methylation (^{m}CG) patterns is essential for chromatin-mediated epigenetic regulation of transcription in plants and mammals. However, functional links between ^{m}CG and other epigenetic mechanisms in vivo remain obscure. Using successive generations of an *Arabidopsis thaliana* mutant deficient in maintaining ^{m}CG, we find that ^{m}CG loss triggers genome-wide activation of alternative epigenetic mechanisms. However, these mechanisms, which involve RNA-directed DNA methylation, inhibiting expression of DNA demethylases, and retargeting of histone H3K9 methylation, act in a stochastic and uncoordinated fashion. As a result, new and aberrant epigenetic patterns are progressively formed over several plant generations in the absence of ^{m}CG. Interestingly, the unconventional redistribution of epigenetic marks is necessary to "rescue" the loss of ^{m}CG, since mutant plants impaired in rescue activities are severely dwarfed and sterile. Our results provide evidence that ^{m}CG is a central coordinator of epigenetic memory that secures stable transgenerational inheritance in plants.

INTRODUCTION

Epigenetic regulation of transcription is accomplished through heritable changes of chromatin properties. Chromatin alterations are associated with a broad range of molecular mechanisms, with DNA methylation and covalent histone modifications being the best characterized. In plants, the spectrum of mechanisms involved in epigenetic regulation appears remarkably complex, exceeding that of mammals. For example, in mammals, methylated cytosines occur almost exclusively in CG sequence contexts, and CG methylation (^{m}CG) patterns are maintained during DNA replication by the maintenance methyltransferase DNA methyltransferase 1 (DNMT1). Similarly, the DNMT1 homolog METHYLTRANSFERASE 1 (MET1) propagates ^{m}CG patterns in plants, but plants also extensively methylate non-CGs. Methylation at CNG (where N = any base) and CHH sites (where H = A, T, or C) is accomplished by the plant-specific methyltransferases CHROMOMETHYLASE 3 (CMT3) and DOMAINS REARRANGED METHYLTRANSFERASE 2 (DRM2), respectively (Chan et al., 2005). DRM2 is the major de novo DNA methyltransferase establishing new cytosine methylation marks in a process directed by short interfering RNAs (siRNAs) termed RNA-directed DNA methylation (RdDM) (Mathieu and Bender, 2004; Matzke and Birchler, 2005). RdDM can methylate cytosines in all sequence contexts. DRM2 and CMT3 have redundant functions in maintaining non-CG methylation at certain loci. Neither *drm2* nor *cmt3* single mutations induce developmental abnormalities, whereas plants lacking both functions have morphological defects (Cao and Jacobsen, 2002; Chan et al., 2006). Importantly, reintroduction of DRM2 and/or CMT3 activity rapidly complements developmental alterations (Chan et al., 2006).

In contrast, perpetuation of ^{m}CG patterns does not involve methyltransferases with redundant functions, and, once altered in mutants, ^{m}CG patterns cannot be restored upon reintroduction of corresponding activities. Deficiencies in ^{m}CG maintenance are deleterious in both mammals and plants. In mice, loss of DNMT1 function leads to early embryonic lethality (Li et al., 1992). In *Arabidopsis*, homozygous partial loss-of-function *met1* mutants are recovered at frequencies as predicted by Mendelian laws (Kankel et al., 2003). However, the number of plants homozygous for the null *met1-3* allele (*met1-3*/*met1-3*; herein termed *met1-3*) is only 2% of the Mendelian prediction for selfed *met1-3*/*MET1* parents (Saze et al., 2003). Since all *met1-3* progeny are uniformly and entirely depleted of ^{m}CG marks, partial lethality cannot be explained by variable loss of ^{m}CG, and the reason for rare survivals of *met1-3* mutants remains unknown.

Lines expressing a *MET1* antisense construct and partial loss-of-function *met1* mutants have relatively mild phenotypes (Finnegan et al., 1996; Kankel et al., 2003; Ronemus et al., 1996); however, *MET1* antisense lines accumulate developmental abnormalities during inbreeding that are correlated with gradual loss of ^{m}CG (Finnegan et al., 1996). A similar progressive accumulation of morphological anomalies occurs in *decrease in DNA methylation 1* (*ddm1*) mutants during repeated self-fertilization (Kakutani et al., 1996). *DDM1* encodes a chromatin-remodeling ATPase of the SNF2/SWI2 family that is required for ^{m}CG maintenance (Brzeski and Jerzmanowski, 2003; Jeddeloh et al., 1999). In early generations of *ddm1* mutants, methylation at heterochromatic centromeric and pericentromeric repeats is preferentially affected, whereas genic regions become affected only in later generations. Such progressive demethylation could explain the gradual accumulation of developmental aberrations during inbreeding of *ddm1* mutants (Kakutani et al., 1996; Vongs et al., 1993). Surprisingly, we routinely observed phenotypic variants among homozygous *met1-3* plants, even though all of these plants are directly depleted of all ^{m}CG. Therefore, the *met1-3* phenotypes cannot be correlated with levels of ^{m}CG.

Here we show that loss of ^{m}CG triggers genome-wide aberrant de novo non-CG methylation by interfering with the RdDM process and expression of DNA demethylases, as well as progressive H3K9 remethylation of heterochromatin. Activation of these epigenetic "backup" mechanisms partially compensates the loss of ^{m}CG marks. However, this "rescue system" acts in a highly uncoordinated and stochastic fashion. Our observations provide an explanation for the low survival of *met1-3* plants, as well as for the stochastic appearance of developmental defects. We suggest that in plants, and possibly in mammals, ^{m}CG evolved not only to provide a level of epigenetic regulation but also to coordinate and stabilize epigenetic memory required for its transgenerational inheritance.

RESULTS

DNA and H3K9 Methylation Patterns Are Unstable in *met1-3*

We previously demonstrated that erasure of ^{m}CG in the null *met1-3* strain (Saze et al., 2003) affects heterochromatic localization of the repressive histone mark H3K9me2 (histone H3 dimethylated at lysine 9; Tariq et al., 2003). To our surprise, the results varied in subsequent *met1-3* generations, with enriched methylated cytosines and H3K9me2 often observed at heterochromatic chromocenters of *met1-3* nuclei (Figures 1A and 1B). Hence, we examined more detailed properties of epigenetic regulation in successive generations of *met1-3* plants, with the first generation indicating a homozygous mutant plant derived from a heterozygous *met1-3*/*MET1* parent and subsequent generation numbers reflecting self-fertilization of homozygous mutants.

DNA methylation and H3K9me2 are highly clustered at heterochromatic chromocenters in wild-type nuclei (Figures 1A and 1B; Soppe et al., 2002; Tariq et al., 2003). Chromocenters of first-generation *met1-3* plant nuclei were depleted of both DNA and H3K9 methylation (Figures 1A and 1B; Tariq et al., 2003). However, in subsequent generations, especially the third and fourth, the DNA and H3K9 methylation signals reappeared at chromocenters (Figures 1A and 1B). Thus, nuclear distribution of DNA methylation and H3K9me2 is markedly unstable in the *met1-3* background, changing rapidly within a few generations.

Inbreeding of *met1-3* Rapidly Aggravates Developmental Defects

Homozygous *met1-3* individuals not only are underrepresented in the progeny of plants heterozygous for *met1-3* (Saze et al., 2003) but also show developmental abnormalities of variable penetrance. These include short plant stature, late flowering, altered flower morphology, and reduced fertility. Further inbreeding of *met1-3* plants increased the frequency and severity of abnormalities (Figure 2A); the fourth generation was generally terminal.

Simultaneously inbred *met1-3* lines showed marked variability in range and severity of phenotype and rate of transgenerational amplification. For example, *met1-3* line 30 showed strong growth inhibition in the first generation, but line 29 showed inhibition only in later generations (Figure 2A and data not shown). Interestingly, recurrent selection to stabilize particular phenotypic traits failed due to the stochastic appearance of a broad range of phenotypes in each *met1-3* generation. For example, "large" and "small" third-generation siblings were self-fertilized and the fourth generation was observed. There was no correlation between parental and progeny phenotypes (Figure 2B), suggesting inherent epigenetic instability in *met1-3*.

Transgenerational Phenotypic Aggravation in *met1-3* Lines Correlates with Progressively Altered Nuclear Architecture

The heterochromatin content (HC) of interphase nuclei from wild-type and *met1-3* plants was measured in successive inbred generations (Figure 2C). HC is expressed as the area and intensity of DAPI-stained chromocenters relative to the entire nucleus. In wild-type plants, 14% of the nucleus was occupied by chromocenters. In first-generation *met1-3* nuclei, chromocenters were clearly visible but HC was only 8.4%. A further HC decrease to 6.1% was found in nuclei of fourth-generation *met1-3* mutants, with typically only 2–3 visible chromocenters (Figure 2C).

Using fluorescence in situ hybridization (FISH), nuclei were categorized into three types according to the signal distribution from a 180 bp centromeric repeat-specific probe (Figure 2D). In type 1 nuclei, the probe hybridized strictly to chromocenters. In type 2 nuclei, part of the hybridization signal was dispersed from chromocenters, and in type 3, the signal was diffuse within the nucleus,

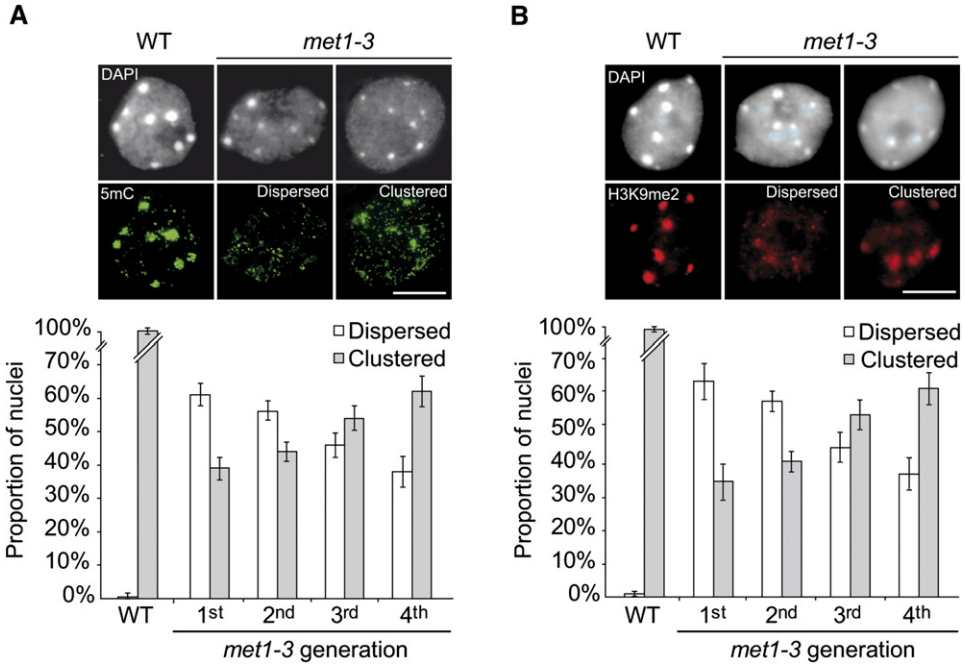

Figure 1. DNA and H3K9 Methylation Patterns Are Unstable in Inbred *met1-3* Homozygous Lines

(A) DNA methylation patterns in wild-type (WT) and successive generations of the *met1-3* mutant analyzed by immunocytology with an antibody against methylated cytosines (5mC). Representative images are shown for WT and two different patterns observed in the *met1-3* third generation, with signal either dispersed from or clustered at chromocenters. The proportions of both nucleus types in WT and *met1-3* plants of the indicated generations were monitored and are represented as a histogram (±SD). Between 261 and 311 nuclei from three independent experiments were scored in each case. Scale bar = 5 μm.

(B) H3K9me2 patterns in WT and successive generations of the *met1-3* mutant analyzed by immunocytology with a specific antibody against this mark. Representative images are shown for WT and two different patterns observed in the *met1-3* third generation, with signals either dispersed from or clustered at chromocenters. The proportions of both nucleus types in WT and *met1-3* plants of the indicated generations were monitored and are represented as a histogram (±SD). Between 260 and 322 nuclei from three independent experiments were scored in each case. Scale bar = 5 μm.

suggesting substantial decondensation of centromeric heterochromatin. Virtually all nuclei of wild-type plants were type 1. In *met1-3* mutants, the proportion of type 1 nuclei decreased gradually upon inbreeding and was replaced by type 2. Type 3 nuclei appeared in the third generation and increased to 23% in the fourth generation (Figure 2D).

Thus, successive *met1-3* inbreeding exacerbates alterations in heterochromatin organization typical of *Arabidopsis*. It is remarkable that the observed restoration of DNA and histone H3K9 methylation during *met1-3* inbreeding correlates inversely with heterochromatin compaction. These unexpected results suggest that repressive marks acquired in the absence of ^{m}CG cannot fully compensate for ^{m}CG depletion.

^{m}CG Controls Proper Targeting of Asymmetrical Methylation

To examine the atypical DNA methylation status appearing during the inbreeding of *met1-3* plants, genomic DNA from different *met1-3* generations was analyzed by DNA gel blot after digestion with cytosine methylation-sensitive restriction endonucleases.

In *met1-3*, 180 bp repeats, 45S rDNA, and pericentromeric *Athila/TSI* repeats all lost CG and CNG methylation at HpaII and MspI sites, respectively (see Figure S1 in the Supplemental Data available with this article online). Indirect effects of *met1* on CNG methylation have been well documented (Saze et al., 2003; for review, see Chan et al., 2005). There was no difference between wild-type and *met1-3* after NlaIII digestion, indicating that neither depletion of ^{m}CG and ^{m}CNG nor the absence of MET1 activity influenced ^{m}CHH levels at these heterochromatic repeats (Figure S1). Therefore, once established in the first *met1-3* generation, the methylation status of these loci is not affected by further inbreeding. In contrast, following reduced CG and CNG methylation at 5S rDNA, CHH methylation increased in successive *met1-3* generations, having already been higher than in wild-type in the first generation (Figure 3A). This was also visualized using HaeIII (in the Columbia accession, the 5S HaeIII site is a CHH). Interestingly, this increased asymmetrical methylation correlated to a partial return of transcriptional silencing at 5S rDNA (Figure 3B; Vaillant et al., 2006). Likewise, a probe corresponding to the *gypsy-class* LTR retroelements revealed progressive, though subtler, increases in

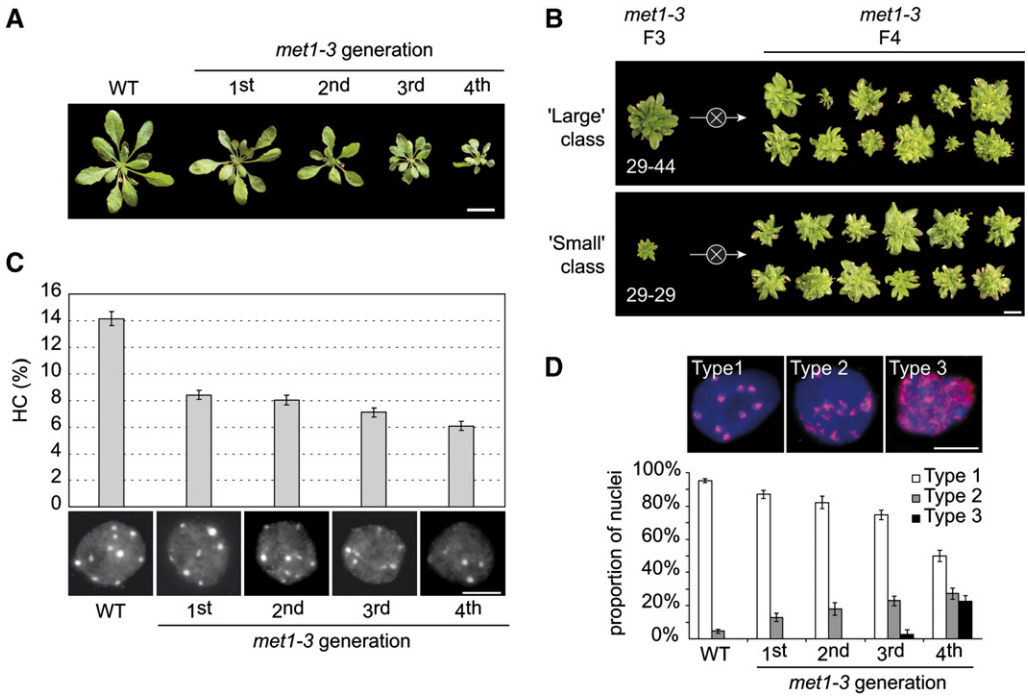

Figure 2. Transgenerational Phenotypic Aggravation and Altered Heterochromatin Structure in *met1-3*

(A) Gradual aggravation of *met1-3* plant phenotype. Representative pictures of 3-week-old WT and *met1-3* plants of the indicated generation are shown. Scale bar = 1.5 cm.

(B) Phenotypic variation observed within fourth-generation siblings. Third-generation *met1-3* siblings with divergent sizes were self-fertilized and compared in size to the fourth-generation progeny. Scale bar = 1.5 cm.

(C) Heterochromatin content (HC) in leaf interphase nuclei from WT and *met1-3* plants of successive generations. Data are presented as percentages (±SEM) and were derived from measuring 60–68 nuclei per entry. Representative nuclei after DAPI staining are shown below each entry. Scale bar = 5 μm.

(D) Progressive alteration of heterochromatin compaction in *met1-3*. Fluorescence in situ hybridization (FISH) analysis was performed using a probe specific for 180 bp centromeric repeats. Nucleus types were categorized according to the fluorescence signal distribution relative to the heterochromatic chromocenters. Data are presented as percentages (±SD) and were derived from measurements of 128–166 nuclei per entry from three independent experiments. Scale bar = 5 μm.

CHH methylation in successive generations of *met1-3* (Figure 3C).

DNA methylation patterns in wild-type and second- and fourth-generation *met1-3* plants were compared further using bisulfite sequencing at specific heterochromatic loci, namely the *gypsy-class* retrotransposon *AtGP1*, the *copia*-like retrotransposon *Ta3*, a 180 bp single repeat, and the *At5g36660* pseudogene. At all loci, ^{m}CG was virtually erased in second- and fourth-generation *met1-3* plants, while CNG methylation was only slightly altered (Figure 4A; the region of the *At5g36660* pseudogene examined is free of CG and CNG sites). At *AtGP1*, the level of ^{m}CHH declined in second-generation *met1-3* plants but increased in the fourth generation, reaching levels higher than in the wild-type (Figure 4; Figure S2). At all loci, de novo methylation appeared ectopically at new cytosine residues in *met1-3*, mainly in asymmetrical contexts (Figure 4A, marked by asterisks). Moreover, these atypical methylation patterns were not faithfully inherited between the second and fourth *met1-3* generations (Figure 4A).

Together, our results suggest that *met1-3* plants gain ectopic CHH methylation at heterochromatic loci following ^{m}CG depletion. Hence, proper ^{m}CG distribution and/or MET1 itself has a critical role in controlling the levels and patterns of non-CG methylation. However, the degree and the kinetics of aberrant CHH methylation vary between targets and *met1-3* inbred lines. For example, in a separate inbred *met1-3* line (line 30), aberrant CHH hypermethylation appearing at 5S rDNA was fixed in the first generation, and further inbreeding had negligible effect (Figure S3).

DNA Methylation Changes in Gene-Rich Chromosomal Regions of *met1-3*

Methylcytosine immunoprecipitation (mCIP) of methylated DNA for methylation profiling of the *Arabidopsis* ATH1 microarray was used to investigate DNA methylation changes within euchromatic regions induced by the *met1-3* mutation upon inbreeding. Results revealed methylation differences in ~28% of genes between the

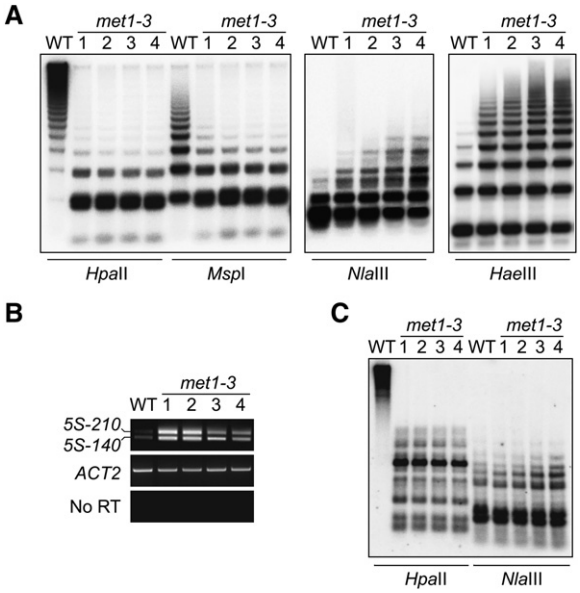

Figure 3. Progressive Hypermethylation of Asymmetrical Cytosines Upon *met1-3* Inbreeding

(A) 5S rDNA hypermethylation at CHH sites. Genomic DNA from WT and successive *met1-3* generations (1–4) digested with HpaII, MspI, NlaIII, or HaeIII was hybridized to a 5S rDNA probe.

(B) Partial transcriptional resilencing at 5S rDNA. RT-PCR detection of 5S-210 and 5S-140 transcript levels measured the release of silencing at 5S repeats. Amplification of *ACTIN 2* (*ACT2*) was used to normalize RNA template amounts. Negative controls (No RT) lacked reverse transcriptase.

(C) Increase in asymmetrical methylation at *gypsy-class* LTR retroelements. Genomic DNA digested with HpaII and NlaIII was hybridized to a *gypsy* probe detecting all *gypsy* elements in the genome.

wild-type and *met1-3* plants (Figure 4B), similar to the previous report of ~33% of genes detected on the *Arabidopsis* tiling microarray (Zhang et al., 2006). Surprisingly, similar proportions of the genes were hypermethylated or hypomethylated in *met1-3*: 8.5% and 9.1%, respectively. For these genes, the DNA methylation changes were conserved between *met1-3* generations. However, progressive methylation changes were observed for a number of genes. In fourth-generation *met1-3* compared with both second-generation *met1-3* and wild-type plants, the observed changes were more frequently due to hypermethylation than to hypomethylation (Figure 4B): progressive hyper- and hypomethylation patterns were detected for 1125 genes (~5.0%) and 562 genes (~2.5%), respectively. Moreover, 2.1% and ~0.7% of the genes profiled were transiently hypermethylated or transiently hypomethylated, respectively, in second-generation *met1-3* compared to wild-type plants (Figure 4B), supporting the dynamic changes in methylation found with bisulfite analysis (Figure 4A). Together, these results show that aberrant de novo DNA methylation in *met1-3* progenies is not restricted to heterochromatin but occurs in a genome-wide manner.

Mechanism of De Novo Methylation in *met1-3*

To examine the possible involvement of RdDM in the aberrant DNA methylation of the *met1-3* genome, we combined *met1-3* and *drm2-2* mutations. DNA gel blot analysis of 5S rDNA after HaeIII digestion showed that hypermethylation of asymmetrical cytosines does not occur in the absence of DRM2 function (Figure 5A). Interestingly, the *drm2-2* single mutation caused a reduction in both CG and CNG methylation at 5S rDNA, although less severe than that in *met1-3* (Figure 5B). These results reveal the contribution of RdDM to the maintenance of CG and non-CG methylation at 5S rDNA loci and demonstrate its decisive role in the acquisition of aberrant CHH methylation in *met1-3*.

siRNA levels corresponding to 5S rRNA genes were drastically increased in *met1-3* plants (Figure 5C; Onodera et al., 2005), indicating that ^{m}CG downregulates siRNA accumulation at these loci. The increased siRNA levels are likely due to the transcriptional derepression in *met1-3*, as illustrated by the overaccumulation of normally silent 5S rRNA transcripts (Figure 3B). Notably, 5S siRNAs were not detected in *drm2-2* or *met1-3 drm2-2* (Figure 5C), suggesting that DRM2 directly or indirectly stabilizes these siRNAs. The requirement for DRM2 and siRNA overaccumulation strongly suggests involvement of the RdDM pathway in aberrant hypermethylation of 5S rDNA loci in *met1-3*.

Importantly, elevated levels of *TSI* siRNAs were also detected in *met1-3* (Figure 5C) despite the fact that *TSI* repeats were not hypermethylated in *met1-3* (Figure 5D). Therefore, overaccumulation of siRNAs is not sufficient for the targeting of de novo DNA methylation. Interestingly, *TSI* siRNA overaccumulation also occurred in the absence of DRM2 (Figure 5C), suggesting functional divergence of siRNAs specific to *TSI* and 5S rDNA.

^{m}CG Is Required for DNA Demethylase Expression

In addition to de novo DNA methylation, increased methylation levels could also result from inhibition of DNA demethylation activity. In *Arabidopsis*, four proteins, REPRESSOR OF SILENCING 1 (ROS1), DEMETER (DME), and DEMETER-LIKE 2 and 3 (DML2/3), have been shown to excise methylated cytosines from DNA (Agius et al., 2006; Gehring et al., 2006; Morales-Ruiz et al., 2006; Penterman et al., 2007).

Low levels of *DML2* and *DML3* transcripts were present in both wild-type and *met1-3* (data not shown). In contrast, *ROS1* transcripts, abundant in the wild-type, were not detectable in *met1-3* by either RT-PCR or RNA gel blots (Figure 6A). *ROS1* transcript accumulation was also strongly downregulated in *drm2-2* and *dcl3-1*. This suggests either that ^{m}CG, which is erased in *met1-3*, is required for *ROS1* transcription or that the aberrant de novo methylation observed in *met1-3* inhibits *ROS1* transcription. To test these alternatives, wild-type and *met1-3* plants were treated with 5-aza-2′-deoxycytidine (5-aza-dC), a DNA methylation inhibitor. *ROS1* expression did not resume in 5-aza-dC-treated *met1-3* plants, while

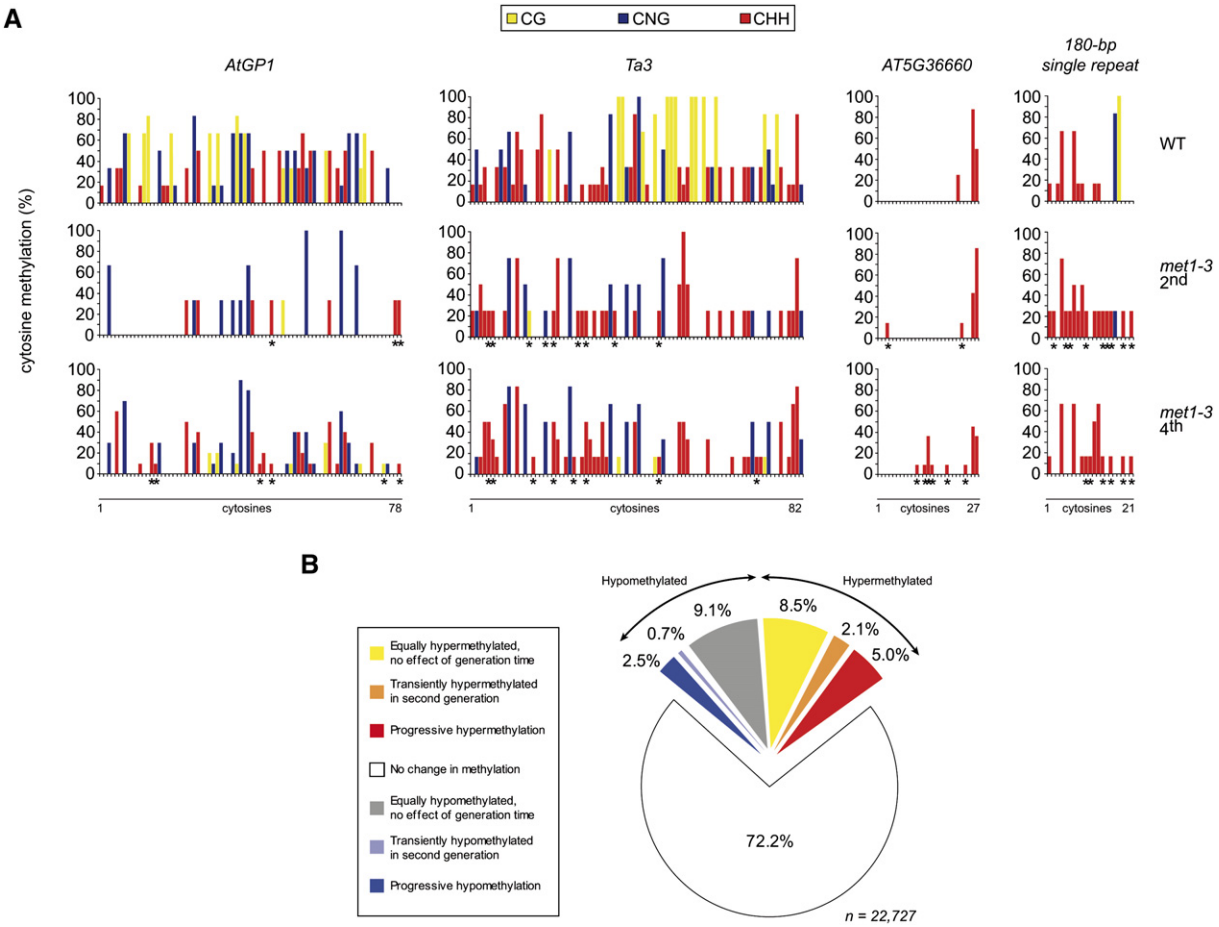

Figure 4. Genome-wide Aberrant De Novo Non-CG Methylation in *met1-3*

(A) *met1-3* alters non-CG methylation patterns at heterochromatic loci. DNA methylation of the indicated heterochromatic sequences in WT plants and plants homozygous for the *met1-3* mutation for two (*met1-3* 2nd) and four generations (*met1-3* 4th) was assayed by bisulfite sequencing. The percentages of methylation of each cytosine residue present along the different sequences analyzed were calculated. Asterisks denote de novo methylated cytosines in *met1-3* plants of either generation relative to WT.

(B) Aberrant de novo methylation within 3′ genic regions revealed by methylcytosine immunoprecipitation analysis on the *Arabidopsis* ATH1 microarray at the 5% false discovery rate. Hypomethylated and hypermethylated patterns represent loss or gain in DNA methylation, respectively, in the *met1-3* generations relative to WT.

transcript accumulation was inhibited in wild-type plants, essentially mimicking *met1-3* (Figure 6B). Therefore, ^{m}CG is required for *ROS1* transcription. Surprisingly, high levels of *DME* transcript were detected in wild-type leaves by both RT-PCR and RNA gel blot (Figures 6A and 6B), challenging a previous observation that *DME* transcription occurs primarily in the central cell of the female gametophyte (Choi et al., 2002). The levels of *DME* transcripts were also downregulated by the loss of ^{m}CG, but not in *drm2-2* or *dcl3-1* (Figures 6A and 6B). In *met1-3*, both *ROS1* expression and *DME* expression were repressed at the transcriptional level as revealed by nuclear run-on assays (Figure 6C). We detected negligible levels of DNA methylation at the *ROS1* promoter region in wild-type and *met1-3* (data not shown). However, previous *Arabidopsis* methylome analysis (Zhang et al., 2006) showed significant gene-body methylation at *ROS1* and *DME* that was erased in *met1-3* (Figure 6D).

Together, these results suggest that maintenance of ^{m}CG is required for expression of DNA demethylases and that transcriptional repression in *met1-3* may contribute to atypical DNA methylation patterns.

CGs Remain Unmethylated in *met1-3* Progeny and Upon Restoration of MET1 Activity

Both RNAi-mediated de novo methylation and hypermethylation in *ros1* mutants have also been shown to affect cytosines residing in CG contexts (Zhu et al., 2007). Moreover, the above results (Figure 5B) demonstrate that a significant part of ^{m}CG at 5S rDNA is determined by persistent RdDM involving DRM2 activity. Therefore, the lack of remethylation at CGs upon *met1-3* inbreeding

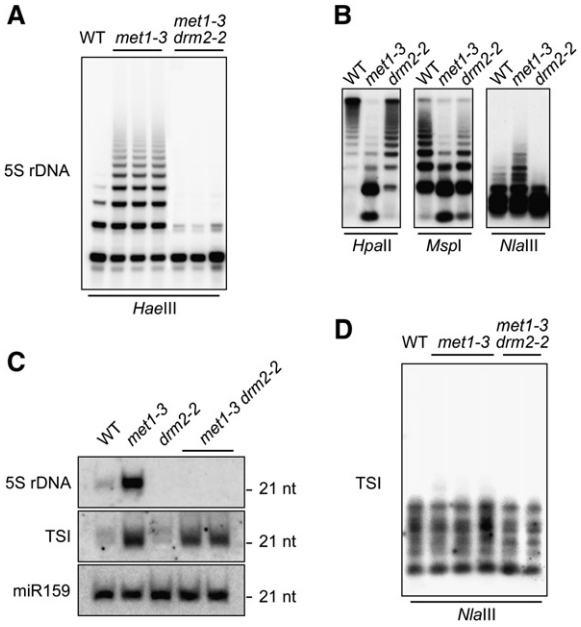

Figure 5. Target-Specific RNAi-Mediated De Novo Methylation Observed in *met1-3*

(A) 5S rDNA hypermethylation at CHH sites requires DRM2. Genomic DNA from one WT, three first-generation *met1-3* single-mutant, and three *met1-3 drm2-2* double-mutant plant siblings was digested with HaeIII and hybridized to a 5S rDNA probe.

(B) *drm2-2* mutation decreases DNA methylation in all sequence contexts at 5S rDNA. Genomic DNA from WT and first-generation *met1-3* and *drm2-2* plants was digested with HpaII, MspI, or HaeIII and hybridized to a 5S rDNA probe.

(C) Accumulation of 5S rDNA and *TSI* siRNAs. Samples from two *met1-3 drm2-2* plants were used. The signal from a miR159 probe was used as a loading control. The position of a 21 nt marker is indicated on the right.

(D) Asymmetrical methylation at *TSI* is not influenced in *met1-3* or *drm2-2*. Genomic DNA from one WT, three *met1-3* first-generation homozygous single-mutant, and two *met1-3 drm2-2* double-mutant plants was digested with NlaIII and hybridized to a *TSI* probe.

was surprising. Although the absence of MET1 activity in *met1-3* could explain the persistence of demethylated CGs, an attractive alternative is the existence of a mechanism preventing CGs from undergoing remethylation.

To distinguish between these two options, *met1-3* plants were backcrossed to the wild-type, and eight *MET1/MET1* F2 individuals were propagated by self-pollination and single-seed descent for seven generations (Figure S5). The Columbia accession of *Arabidopsis* carries three major unlinked 5S rDNA clusters; thus, the wild-type or *met1-3*-derived loci independently segregated in these *MET1/MET1* lines. The clearly demethylated CGs found in three of these *MET1/MET1* lines after seven generations (Figure S5) can only be explained by the segregation of persistently demethylated 5S rDNA loci derived from the original *met1-3* parent. Such steady CG hypomethylation retention through transgenerational inheritance in the form of demethylated CGs suggests that, once demethylated in *met1-3*, the CGs remain hypomethylated even in the presence of ^{m}CG maintenance activity. In contrast, CG remethylation of hypomethylated sequences in *met1* partial loss-of-function mutants or *MET1* antisense lines occurs when MET1 function is restored (Kankel et al., 2003; Ronemus et al., 1996), suggesting that residual ^{m}CG is a prerequisite for the reestablishment of ^{m}CG patterns. Given evidence that MET1 is involved in de novo CG methylation (Aufsatz et al., 2004) and that DRM2 contributes significantly to ^{m}CG at 5S rDNA (Figure 5D), our results support the hypothesis of active protection of CGs from remethylation once they have completely lost their methylation in *met1-3*.

Retargeting of H3K9me2 to Heterochromatin by a DNA Methylation-Independent Mechanism

Similar nuclear distribution of DNA methylation and H3K9me2 was observed in successive generations of *met1-3* (Figures 1A and 1B), suggesting that the ectopically appearing non-CG methylation directs H3K9me2 in the absence of ^{m}CG.

To address this question at the DNA sequence level, we assayed H3K9me2 distribution by chromatin immunoprecipitation (ChIP) at loci used for determining DNA methylation. For all heterochromatic loci, there was a drastic reduction in H3K9me2 in second-generation *met1-3* plants (Figure S6). In the fourth generation, all loci were clearly enriched in H3K9me2 compared with the second generation. Importantly, some loci remained demethylated upon *met1-3* inbreeding (e.g., 180 bp repeats, 45S rDNA, and *TSI*; Figure S1), suggesting that H3K9me2 accumulation may occur independently of DNA methylation changes.

Biological Consequences of the Aberrant DNA Methylation and H3K9 Remethylation in *met1-3*

The biological consequences of aberrant non-CG methylation and H3K9 remethylation during *met1-3* inbreeding were examined by introducing either *drm2-2* or *kyp-7* mutations into *met1-3*. KYP is the major H3K9 methyltransferase in *Arabidopsis* (Jackson et al., 2004). If acquisition of methylation aggravates phenotypic abnormalities, double-mutant plants should show improved fitness over the *met1-3* single mutant. Conversely, if these marks "compensate" for ^{m}CG loss in *met1-3*, early generations of double mutants should display severe abnormalities. Importantly, neither *drm2-2* nor *kyp-7* homozygous plants displayed morphological defects, even after eight generations of self-fertilization (data not shown).

By the first generation, homozygous double-mutant plants exhibited more acute abnormalities than *met1-3* siblings (Figure 7A). The growth and fertility of *met1-3 drm2-2* plants was drastically reduced, while *met1-3 kyp-7* plants were completely sterile and strongly dwarfed. Transcript analysis of heterochromatic sequences, such as 180 bp and *106B* repeats and the *Ta3* retrotransposon, revealed RNA overaccumulation in each double mutant relative to the *met1-3* single mutant (Figure 7B). Notably, transcripts of the MULE transposon

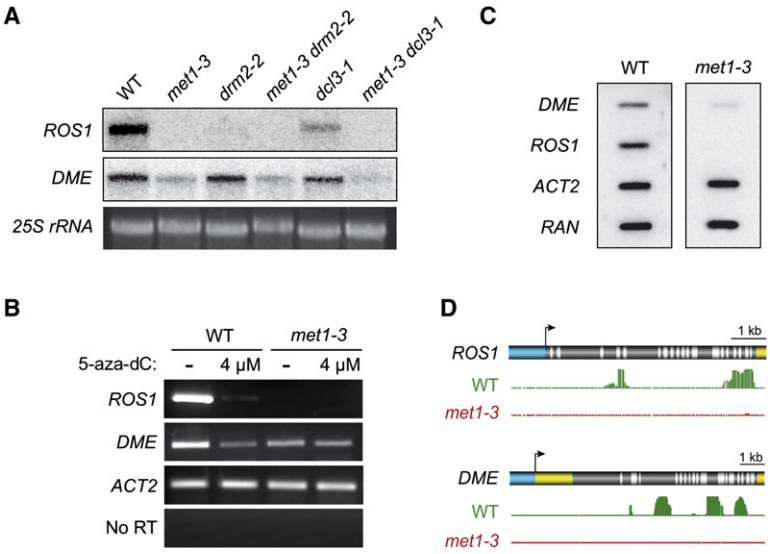

Figure 6. ^{m}CG Is Required for *ROS1* and *DME* Expression

(A) *ROS1* and *DME* mRNA accumulation was determined by RNA gel blot analysis with 10 μg of total RNA from 3-week-old leaves of the indicated plant genotypes. The blot was hybridized to probes corresponding to *ROS1* and *DME*.

(B) 5-aza-dC treatment repressed transcription of *ROS1* and *DME*. *ROS1* and *DME* transcripts were detected by RT-PCR. Amplification of *ACTIN 2* (*ACT2*) was used to normalize RNA template amounts. Negative controls (No RT) lacked reverse transcriptase.

(C) Nuclear run-on assay showing transcriptional repression of *ROS1* and *DME* in *met1-3*. *ACT2* and *RAN* (which encodes a small GTP-binding protein) genes were used as controls.

(D) DNA methylation profiles of *ROS1* and *DME* in WT and *met1-3* represented from the publicly available database http://signal.salk.edu/cgi-bin/methylome (Zhang et al., 2006). Promoters (blue), untranslated regions (yellow), exons (black), introns (white), and transcription start sites (arrows) are shown.

At1g40097 were detected in *met1-3 kyp-7*, but not in *met1-3 drm2-2* or any single mutant (Figure 7B). Thus, a particular combination of repressive marks would determine locus-specific mechanisms of epigenetic regulation involving mainly ^{m}CGs or MET1, non-CG methylation or DRM2, H3K9me2 or KYP, or combinations thereof.

The compaction of centromeric 180 bp repeats and 5S rDNA was lost in double mutants (Figure 7C). In *met1-3*

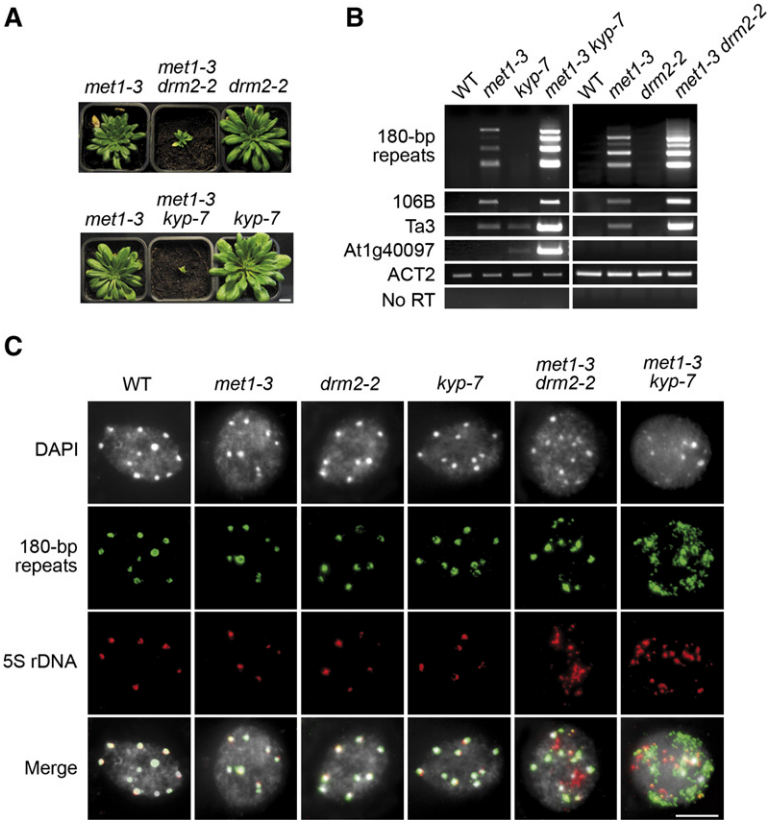

Figure 7. DRM2 and KYP Contribute to the "Rescue" of ^{m}CG Loss in *met1-3*

(A) *met1-3 drm2-2* and *met1-3 kyp-7* double mutants displayed more severe phenotypes than the respective single mutants. Representative images of 3-week-old siblings segregating from *met1-3/MET1 drm2-2/DRM2* and *met1-3/MET1 kyp-7/KYP* parents are shown. Scale bar = 1 cm.

(B) Synergistic release of transcription at heterochromatic loci. Transcripts were detected by RT-PCR. Amplification of *ACTIN 2* (*ACT2*) was used to normalize RNA template amounts. Negative controls (No RT) lacked reverse transcriptase.

(C) Alteration of heterochromatic repeat organization in *met1-3 drm2-2* and *met1-3 kyp-7* double mutants. FISH analysis was performed on nuclei from 3-week-old rosette leaves of the indicated genotypes simultaneously with probes specific to 180 bp centromeric repeats (green) and 5S rDNA (red). Scale bar = 5 μm.

drm2-2, primarily 5S rDNA loci were affected, while the structure of both repeat types was significantly relaxed in *met1-3 kyp-7*. Therefore, profound phenotypic aggravation, possibly through synergistic release of silencing and accelerated changes in nuclear architecture, in *met1-3 drm2-2* and *met1-3 kyp-7* strongly indicates contributions by DRM2 and KYP toward the "rescue" of ^{m}CG loss in *met1-3*.

DISCUSSION

H3K9me2 marks are relocated away from heterochromatic chromocenters in the absence of ^{m}CG (Soppe et al., 2002; Tariq et al., 2003). It was expected that this state would be stable and that only restoration of ^{m}CG would reset H3K9 methylation. Here, we show that in the absence of ^{m}CG, epigenetic stability cannot be achieved since the remaining epigenetic mechanisms, such as non-CG methylation and H3K9 methylation, start to operate in a highly stochastic fashion. This leads to transgenerationally progressive de novo deposition of these marks, even at previously unmarked locations. It was previously reported that the floral homeotic genes *SUPERMAN* and *AGAMOUS* become ectopically hypermethylated in *met1* partial loss-of-function mutants and in *MET1* antisense lines (Jacobsen and Meyerowitz, 1997; Jacobsen et al., 2000). At these loci, de novo methylation also occurred mainly at asymmetric sites. Thus far, the mechanism underlying this counterintuitive and possibly local hypermethylation has remained unclear. Here, we provide evidence that de novo non-CG methylation, triggered by ^{m}CG erasure, occurs genome-wide and affects many heterochromatic and genic loci. The new methylation patterns are formed stochastically and are irregularly inherited. Thus, the continual maintenance of ^{m}CG patterns is the key factor in controlling transgenerational inheritance of epigenetic information, including proper guidance of H3K9me2 and non-CG methylation. Mechanistically, in the absence of native ^{m}CG, RdDM becomes misdirected and genes encoding DNA demethylase activities (*ROS1*, *DME*) are repressed. Interestingly, both processes appear to be closely interwoven since mutations in components of the RdDM pathway, such as *DCL3* (Figure 6A) and *NRPD2a* (data not shown; Huettel et al., 2006), downregulate levels of *ROS1* transcripts.

ROS1 transcript levels are also reduced in the partial loss-of-function mutant allele *met1-1* (Huettel et al., 2006). Furthermore, analysis of this mutant revealed that decreased density of ^{m}CG impacts siRNA levels, causing either a decrease (Lippman et al., 2003, 2004) or the overaccumulation of siRNAs at different loci (Figure 7; Onodera et al., 2005). Just how ^{m}CG influences siRNA levels remains unclear since the loss of ^{m}CG releases transcriptional silencing at all examined loci, thereby increasing the amounts of primary transcripts that can be processed into siRNAs. Consequently, the loss of ^{m}CG must influence siRNA levels posttranscriptionally, most likely by modulating the RDR2-DCL3-dependent siRNA biogenesis pathway, the main siRNA generator in *Arabidopsis* (Kasschau et al., 2007). In turn, siRNA levels may affect distribution of non-CG methylation, which influences siRNA biogenesis. Such locus-specific regulatory feedback loops may create variability and irregular transmission of methylation patterns at affected loci as observed here. Remarkably, no aberrant DNA methylation was observed at certain loci such as *TSI*, despite overaccumulation of the corresponding siRNAs in *met1-3*. Thus, elevated amounts of siRNAs are not automatically channeled to the RdDM pathway, suggesting that the 24 nt siRNAs are functionally specialized into subclasses that may or may not trigger DNA methylation.

ROS1, and possibly DME, can trim the genome of excess methylation (Zhu et al., 2007), and *ros1* mutants gradually acquire abnormal phenotypes upon inbreeding (Gong et al., 2002). Thus, depletion of *ROS1* and *DME* transcripts in *met1-3* certainly contributes to transgenerational alteration of DNA methylation. Moreover, non-CG methylation patterns at *AtGP1* are altered to a similar extent in *met1-3* and *ros1-1* (Figure 4; Figure S2; Zhu et al., 2007). This implies that, at this locus, suppression of demethylase activities rather than alteration of RdDM contributes to the atypical DNA methylation patterns in *met1-3*. Consistent with this conclusion, the depletion of ^{m}CG in *met1* has no influence on *AtGP1* siRNA levels (Lippman et al., 2003).

Only ~2% of the expected numbers of homozygous *met1-3* individuals were recovered from self-fertilized heterozygous *met1-3/MET1* plants. Considering the stochasticity in the distribution of de novo repressive marks (non-CG methylation and H3K9me2) in the absence of MET1 and ^{m}CG, it is possible that only particular patterns of these marks allow survival of an individual. It has been shown that non-CG methylation and H3K9 methylation modulate transcription of genes involved in developmental decisions in *Arabidopsis* (Chan et al., 2006; Zhang et al., 2006). The severe developmental deficiencies and sterility of *met1-3 drm2-2* and *met1-3 kyp-7* double mutants confirm the decisive role of both suppressive marks for *met1-3* viability. Notably, the rapid and drastic decompaction of chromocenters observed in the absence of DRM2 and KYP activities suggests that non-CG and H3K9 methylation slows heterochromatin decomposition in *met1-3*.

In late *met1-3* generations, all heterochromatic sequences examined returned to wild-type H3K9me2 levels. Once depleted of DNA methylation in early *met1-3* generations, some of these sequences also remain hypomethylated in later generations despite H3K9me2 recovery. Therefore, retargeting of H3K9me2 seems to involve a DNA methylation-independent mechanism. Such a mechanism has been postulated for human cancer cells in which DNA methylation is erased by disrupting the DNA methyltransferase genes *DNMT1* and *DNMT3b*. In these cells, silencing of the tumor suppressor gene $p16^{INK4a}$ is eliminated, and H3K9me2 is lost at this gene (Bachman et al., 2003; Rhee et al., 2002). Interestingly, after

continued passage of such cells, H3K9 remethylation occurs in conjunction with resilencing of *p16*^{INK4a}, but in the absence of DNA methylation (Bachman et al., 2003). Therefore, both plants and mammals possess alternative mechanisms that restore H3K9me2 independently of DNA methylation. In *Arabidopsis*, the involvement of H3K27me1 and H3K27me2 marks persisting in heterochromatin independently of DNA methylation (Mathieu et al., 2005) would be an attractive explanation. However, there is as yet no experimental evidence for this since *Arabidopsis* mutations affecting heterochromatic distribution of H3K27me1 and H3K27me2 have not been isolated.

Remarkably, loci like 5S rDNA that regain H3K9me2 and non-CG methylation in late *met1-3* generations remain depleted of ^{m}CG for many plant generations, even upon return of MET1 activity. This is consistent with previous observations of the persistence of CG hypomethylation at some loci when *met1* and *ddm1* mutants are outcrossed to wild-type (Kakutani et al., 1999; Kankel et al., 2003; Lippman et al., 2004). It has been proposed that this illustrates a *cis*-preference of siRNA-directed de novo methylation (Zilberman and Henikoff, 2005). This hypothesis is supported by the suppression of the accumulation of some endogenous siRNAs by partial loss-of-function *met1* mutations (Lippman et al., 2003), pointing toward a requirement for DNA methylation in siRNA production. However, a *cis*-preference for RdDM does not explain our observations that RdDM, contributing to maintenance of ^{m}CG at 5S rDNA in wild-type plants, does not cause CG remethylation in *met1-3* even though 5S siRNAs levels are drastically elevated. Although a preference for DRM2-mediated de novo methylation toward non-CGs (Wada et al., 2003) may contribute to the persistence of demethylated CGs, it is unlikely to account for preventing CG remethylation over many plant generations. Thus, an active protection mechanism preventing remethylation of CGs should be considered, as suggested for mammals, in which methylation patterns are reestablished at about the time of embryo implantation. At this stage, although the entire genome is subject to de novo methylation, a subset of CG islands is specifically protected from modification due to *cis*-elements binding the specificity protein 1 (SP1; Brandeis et al., 1994). Alternatively, protection of CGs against methylation might also be achieved by proteins preferentially binding to nonmethylated CGs. For instance, the CXXC domain of several mammalian chromatin-associated proteins efficiently binds to nonmethylated CGs (Birke et al., 2002; Jorgensen et al., 2004; Lee et al., 2001). Plant proteins with similar activities remain to be characterized.

Taken together, our results suggest that ^{m}CG not only orchestrates distribution of non-CG and H3K9 methylation but also is essential for stable transgenerational inheritance of epigenetic information. The presence and functional separation of CG and non-CG methylation is unique to plants. The sessile lifestyle of plants requires efficient adaptation to environmental changes. We propose that immediate, nonheritable stress responses may be associated with alteration of non-CG methylation patterns mediated by siRNAs/RdDM and ROS1/DME, while long-term, heritable adaptation of plant populations to a changing environment would require modulation of ^{m}CG patterns.

EXPERIMENTAL PROCEDURES

Plant Material and 5-aza-dC Treatment

Plants were grown in soil under short-day conditions (8 hr light/16 hr dark) at 22°C. The *met1-3* and *dcl3-1* strains have been described previously (Saze et al., 2003; Xie et al., 2004). The *drm2-2* (Chan et al., 2006) and *kyp-7* T-DNA insertion lines (SALK_150863 and SALK_069326, respectively) were obtained from the Salk Institute Genomic Analysis Laboratory. T-DNA insertion in *drm2-2* is in the predicted methyltransferase domain of *DRM2* and would be expected to create a null mutation (Chan et al., 2006). *KYP* mRNA was not detected in *kyp-7* mutants after 30 cycles of RT-PCR (data not shown); therefore, *kyp-7* is expected to be a null mutant. *met1-3*, *drm2-2*, *kyp-7*, and *dcl3-1* are all in the Columbia (Col-0) genetic background. The *ros1-1* mutant is in the C24 background and has been described previously (Gong et al., 2002). For 5-aza-dC treatment, seeds were germinated and grown for 9 days on 1/2 MS medium containing 4 μM 5-aza-dC (Sigma).

FISH and Immunocytology

FISH was performed on young rosette leaves as previously described (Probst et al., 2003). A 5-methylcytosine-specific antibody was used for immunostaining of methylated DNA (dilution 1:50; Eurogentec). Immunodetection of H3K9me2 was performed with young rosette leaves as described previously (Mathieu et al., 2005) using an antibody specific for dimethyl H3K9 (dilution 1:100; Perez-Burgos et al., 2004). Images were analyzed with a Zeiss Axioplan 2 microscope equipped with a cooled charge-coupled device camera. Images were merged and processed using Adobe Photoshop.

ChIP

ChIP was performed as described previously (Mathieu et al., 2005). The histone-DNA complexes were immunoprecipitated with α-dimethyl H3K9 (Perez-Burgos et al., 2004). All PCR reactions were performed in 20 μl final volume, starting with 5 min at 95°C and followed by 21–40 cycles (depending on the region being amplified) of 95°C, 60°C (50°C for 45S rDNA; 54°C for 5S rDNA), and 72°C (30 s each) with a final elongation of 5 min at 72°C. PCR products were separated on 3% agarose gels.

DNA and RNA Gel Blot Analysis

DNA gel blot analysis was performed as described previously (Vaillant et al., 2006). Total RNA was extracted from 3-week-old leaves using TRI Reagent (Sigma). RNA gel blot analysis was performed as described previously (Steimer et al., 2000). Probes were labeled with [α-^{32}P]dCTP using random hexamer priming (Megaprime DNA labeling system, Amersham). For small RNA detection, 15 μg of total RNA was used as described previously (Dunoyer et al., 2004). siRNA1003 (5S rDNA) and miR159 were detected using end-labeled DNA oligonucleotides (Xie et al., 2004). For detecting the *TSI* small RNAs, the *TSI-A15* probe was labeled using random hexamer priming. Nuclear run-on assays were carried out starting from 10 g of seedlings as described previously (Van Blokland et al., 1994).

Methylated DNA Immunoprecipitation, Microarray Analysis, and Bisulfite Genomic Sequencing

See Supplemental Experimental Procedures.

Expression Analysis

Aliquots of 3 μg of total RNA were treated with RQ1 DNase (Promega), and 100 ng of DNase-treated total RNA was used as input in

semiquantitative RT-PCR reactions using the OneStep RT-PCR Kit (QIAGEN). Controls were performed without reverse transcriptase to detect contaminating DNA. Amplification of *ACTIN2* RNA was used as an internal control. PCR conditions and primers are described in Supplemental Experimental Procedures.

Supplemental Data

Supplemental Data include Supplemental Experimental Procedures, Supplemental References, and six figures and can be found with this article online at http://www.cell.com/cgi/content/full/130/5/851/DC1/.

ACKNOWLEDGMENTS

We thank P. King for helpful comments on the manuscript and members of the Paszkowski lab for stimulating discussions. We thank D. Schübeler and G. Theiler for assisting with the mCIP analysis, J.K. Zhu for providing the *ros1-1* mutant, O. Mittelsten Scheid for run-on protocols and advice, and P. Dunoyer and O. Voinnet for help with small RNA detection. This work was supported by grants from the Swiss National Science Foundation (3100A0-102107), the European Commission through The Epigenome Network of Excellence (LSHG-CT-2004-503433), and the Targeted Gene Integration in Plants consortium (018785).

Received: March 13, 2007
Revised: May 24, 2007
Accepted: July 6, 2007
Published: September 6, 2007

REFERENCES

Agius, F., Kapoor, A., and Zhu, J.K. (2006). Role of the Arabidopsis DNA glycosylase/lyase ROS1 in active DNA demethylation. Proc. Natl. Acad. Sci. USA *103*, 11796–11801.

Aufsatz, W., Mette, M.F., Matzke, A.J., and Matzke, M. (2004). The role of MET1 in RNA-directed de novo and maintenance methylation of CG dinucleotides. Plant Mol. Biol. *54*, 793–804.

Bachman, K.E., Park, B.H., Rhee, I., Rajagopalan, H., Herman, J.G., Baylin, S.B., Kinzler, K.W., and Vogelstein, B. (2003). Histone modifications and silencing prior to DNA methylation of a tumor suppressor gene. Cancer Cell *3*, 89–95.

Birke, M., Schreiner, S., Garcia-Cuellar, M.P., Mahr, K., Titgemeyer, F., and Slany, R.K. (2002). The MT domain of the proto-oncoprotein MLL binds to CpG-containing DNA and discriminates against methylation. Nucleic Acids Res. *30*, 958–965.

Brandeis, M., Frank, D., Keshet, I., Siegfried, Z., Mendelsohn, M., Nemes, A., Temper, V., Razin, A., and Cedar, H. (1994). Sp1 elements protect a CpG island from de novo methylation. Nature *371*, 435–438.

Brzeski, J., and Jerzmanowski, A. (2003). Deficient in DNA methylation 1 (DDM1) defines a novel family of chromatin-remodeling factors. J. Biol. Chem. *278*, 823–828.

Cao, X., and Jacobsen, S.E. (2002). Locus-specific control of asymmetric and CpNpG methylation by the DRM and CMT3 methyltransferase genes. Proc. Natl. Acad. Sci. USA *99* (*Suppl 4*), 16491–16498.

Chan, S.W., Henderson, I.R., and Jacobsen, S.E. (2005). Gardening the genome: DNA methylation in Arabidopsis thaliana. Nat. Rev. Genet. *6*, 351–360.

Chan, S.W., Henderson, I.R., Zhang, X., Shah, G., Chien, J.S., and Jacobsen, S.E. (2006). RNAi, DRD1, and histone methylation actively target developmentally important non-CG DNA methylation in arabidopsis. PLoS Genet. *2*, e83.

Choi, Y., Gehring, M., Johnson, L., Hannon, M., Harada, J.J., Goldberg, R.B., Jacobsen, S.E., and Fischer, R.L. (2002). DEMETER, a DNA glycosylase domain protein, is required for endosperm gene imprinting and seed viability in arabidopsis. Cell *110*, 33–42.

Dunoyer, P., Lecellier, C.H., Parizotto, E.A., Himber, C., and Voinnet, O. (2004). Probing the microRNA and small interfering RNA pathways with virus-encoded suppressors of RNA silencing. Plant Cell *16*, 1235–1250.

Finnegan, E.J., Peacock, W.J., and Dennis, E.S. (1996). Reduced DNA methylation in Arabidopsis thaliana results in abnormal plant development. Proc. Natl. Acad. Sci. USA *93*, 8449–8454.

Gehring, M., Huh, J.H., Hsieh, T.F., Penterman, J., Choi, Y., Harada, J.J., Goldberg, R.B., and Fischer, R.L. (2006). DEMETER DNA glycosylase establishes MEDEA polycomb gene self-imprinting by allele-specific demethylation. Cell *124*, 495–506.

Gong, Z., Morales-Ruiz, T., Ariza, R.R., Roldan-Arjona, T., David, L., and Zhu, J.K. (2002). ROS1, a repressor of transcriptional gene silencing in Arabidopsis, encodes a DNA glycosylase/lyase. Cell *111*, 803–814.

Huettel, B., Kanno, T., Daxinger, L., Aufsatz, W., Matzke, A.J., and Matzke, M. (2006). Endogenous targets of RNA-directed DNA methylation and Pol IV in Arabidopsis. EMBO J. *25*, 2828–2836.

Jackson, J.P., Johnson, L., Jasencakova, Z., Zhang, X., PerezBurgos, L., Singh, P.B., Cheng, X., Schubert, I., Jenuwein, T., and Jacobsen, S.E. (2004). Dimethylation of histone H3 lysine 9 is a critical mark for DNA methylation and gene silencing in Arabidopsis thaliana. Chromosoma *112*, 308–315.

Jacobsen, S.E., and Meyerowitz, E.M. (1997). Hypermethylated SUPERMAN epigenetic alleles in arabidopsis. Science *277*, 1100–1103.

Jacobsen, S.E., Sakai, H., Finnegan, E.J., Cao, X., and Meyerowitz, E.M. (2000). Ectopic hypermethylation of flower-specific genes in Arabidopsis. Curr. Biol. *10*, 179–186.

Jeddeloh, J.A., Stokes, T.L., and Richards, E.J. (1999). Maintenance of genomic methylation requires a SWI2/SNF2-like protein. Nat. Genet. *22*, 94–97.

Jorgensen, H.F., Ben-Porath, I., and Bird, A.P. (2004). Mbd1 is recruited to both methylated and nonmethylated CpGs via distinct DNA binding domains. Mol. Cell. Biol. *24*, 3387–3395.

Kakutani, T., Jeddeloh, J.A., Flowers, S.K., Munakata, K., and Richards, E.J. (1996). Developmental abnormalities and epimutations associated with DNA hypomethylation mutations. Proc. Natl. Acad. Sci. USA *93*, 12406–12411.

Kakutani, T., Munakata, K., Richards, E.J., and Hirochika, H. (1999). Meiotically and mitotically stable inheritance of DNA hypomethylation induced by ddm1 mutation of Arabidopsis thaliana. Genetics *151*, 831–838.

Kankel, M.W., Ramsey, D.E., Stokes, T.L., Flowers, S.K., Haag, J.R., Jeddeloh, J.A., Riddle, N.C., Verbsky, M.L., and Richards, E.J. (2003). Arabidopsis MET1 cytosine methyltransferase mutants. Genetics *163*, 1109–1122.

Kasschau, K.D., Fahlgren, N., Chapman, E.J., Sullivan, C.M., Cumbie, J.S., Givan, S.A., and Carrington, J.C. (2007). Genome-wide profiling and analysis of Arabidopsis siRNAs. PLoS Biol. *5*, e57.

Lee, J.H., Voo, K.S., and Skalnik, D.G. (2001). Identification and characterization of the DNA binding domain of CpG-binding protein. J. Biol. Chem. *276*, 44669–44676.

Li, E., Bestor, T.H., and Jaenisch, R. (1992). Targeted mutation of the DNA methyltransferase gene results in embryonic lethality. Cell *69*, 915–926.

Lippman, Z., May, B., Yordan, C., Singer, T., and Martienssen, R. (2003). Distinct mechanisms determine transposon inheritance and methylation via small interfering RNA and histone modification. PLoS Biol. *1*, E67.

Lippman, Z., Gendrel, A.V., Black, M., Vaughn, M.W., Dedhia, N., McCombie, W.R., Lavine, K., Mittal, V., May, B., Kasschau, K.D.,

et al. (2004). Role of transposable elements in heterochromatin and epigenetic control. Nature *430*, 471–476.

Mathieu, O., and Bender, J. (2004). RNA-directed DNA methylation. J. Cell Sci. *117*, 4881–4888.

Mathieu, O., Probst, A.V., and Paszkowski, J. (2005). Distinct regulation of histone H3 methylation at lysines 27 and 9 by CpG methylation in Arabidopsis. EMBO J. *24*, 2783–2791.

Matzke, M.A., and Birchler, J.A. (2005). RNAi-mediated pathways in the nucleus. Nat. Rev. Genet. *6*, 24–35.

Morales-Ruiz, T., Ortega-Galisteo, A.P., Ponferrada-Marin, M.I., Martinez-Macias, M.I., Ariza, R.R., and Roldan-Arjona, T. (2006). DEMETER and REPRESSOR OF SILENCING 1 encode 5-methylcytosine DNA glycosylases. Proc. Natl. Acad. Sci. USA *103*, 6853–6858.

Onodera, Y., Haag, J.R., Ream, T., Nunes, P.C., Pontes, O., and Pikaard, C.S. (2005). Plant nuclear RNA polymerase IV mediates siRNA and DNA methylation-dependent heterochromatin formation. Cell *120*, 613–622.

Penterman, J., Zilberman, D., Huh, J.H., Ballinger, T., Henikoff, S., and Fischer, R.L. (2007). DNA demethylation in the Arabidopsis genome. Proc. Natl. Acad. Sci. USA *104*, 6752–6757.

Perez-Burgos, L., Peters, A.H., Opravil, S., Kauer, M., Mechtler, K., and Jenuwein, T. (2004). Generation and characterization of methyl-lysine histone antibodies. Methods Enzymol. *376*, 234–254.

Probst, A.V., Fransz, P.F., Paszkowski, J., and Mittelsten Scheid, O. (2003). Two means of transcriptional reactivation within heterochromatin. Plant J. *33*, 743–749.

Rhee, I., Bachman, K.E., Park, B.H., Jair, K.W., Yen, R.W., Schuebel, K.E., Cui, H., Feinberg, A.P., Lengauer, C., Kinzler, K.W., et al. (2002). DNMT1 and DNMT3b cooperate to silence genes in human cancer cells. Nature *416*, 552–556.

Ronemus, M.J., Galbiati, M., Ticknor, C., Chen, J., and Dellaporta, S.L. (1996). Demethylation-induced developmental pleiotropy in Arabidopsis. Science *273*, 654–657.

Saze, H., Mittelsten Scheid, O., and Paszkowski, J. (2003). Maintenance of CpG methylation is essential for epigenetic inheritance during plant gametogenesis. Nat. Genet. *34*, 65–69.

Soppe, W.J., Jasencakova, Z., Houben, A., Kakutani, T., Meister, A., Huang, M.S., Jacobsen, S.E., Schubert, I., and Fransz, P.F. (2002). DNA methylation controls histone H3 lysine 9 methylation and heterochromatin assembly in Arabidopsis. EMBO J. *21*, 6549–6559.

Steimer, A., Amedeo, P., Afsar, K., Fransz, P., Mittelsten Scheid, O., and Paszkowski, J. (2000). Endogenous targets of transcriptional gene silencing in Arabidopsis. Plant Cell *12*, 1165–1178.

Tariq, M., Saze, H., Probst, A.V., Lichota, J., Habu, Y., and Paszkowski, J. (2003). Erasure of CpG methylation in Arabidopsis alters patterns of histone H3 methylation in heterochromatin. Proc. Natl. Acad. Sci. USA *100*, 8823–8827.

Vaillant, I., Schubert, I., Tourmente, S., and Mathieu, O. (2006). MOM1 mediates DNA-methylation-independent silencing of repetitive sequences in Arabidopsis. EMBO Rep. *7*, 1273–1278.

Van Blokland, R., Van der Geest, N., Mol, J.N.M., and Kooter, J.M. (1994). Transgene-mediated suppression of chalcone synthase expression in Petunia hybrida results from an increase in RNA turnover. Plant J. *6*, 861–877.

Vongs, A., Kakutani, T., Martienssen, R.A., and Richards, E.J. (1993). Arabidopsis thaliana DNA methylation mutants. Science *260*, 1926–1928.

Wada, Y., Ohya, H., Yamaguchi, Y., Koizumi, N., and Sano, H. (2003). Preferential de novo methylation of cytosine residues in non-CpG sequences by a domains rearranged DNA methyltransferase from tobacco plants. J. Biol. Chem. *278*, 42386–42393.

Xie, Z., Johansen, L.K., Gustafson, A.M., Kasschau, K.D., Lellis, A.D., Zilberman, D., Jacobsen, S.E., and Carrington, J.C. (2004). Genetic and functional diversification of small RNA pathways in plants. PLoS Biol. *2*, E104.

Zhang, X., Yazaki, J., Sundaresan, A., Cokus, S., Chan, S.W., Chen, H., Henderson, I.R., Shinn, P., Pellegrini, M., Jacobsen, S.E., and Ecker, J.R. (2006). Genome-wide high-resolution mapping and functional analysis of DNA methylation in arabidopsis. Cell *126*, 1189–1201.

Zhu, J., Kapoor, A., Sridhar, V.V., Agius, F., and Zhu, J.K. (2007). The DNA glycosylase/lyase ROS1 functions in pruning DNA methylation patterns in Arabidopsis. Curr. Biol. *17*, 54–59.

Zilberman, D., and Henikoff, S. (2005). Epigenetic inheritance in Arabidopsis: selective silence. Curr. Opin. Genet. Dev. *15*, 557–562.

Accession Numbers

Microarray data described herein can be downloaded from the Gene Expression Omnibus (http://www.ncbi.nlm.nih.gov/geo/) under the accession number GSE8279.